Evidence of a Pressure-Induced Metallization Process in Monoclinic VO_2

E. Arcangeletti,[1] L. Baldassarre,[1] D. Di Castro,[1] S. Lupi,[1] L. Malavasi,[2] C. Marini,[1] A. Perucchi,[1] and P. Postorino[1]

[1]*"Coherentia" CNR-INFM and Dipartimento di Fisica, Università di Roma La Sapienza, Piazzale Aldo Moro 2, I-00185 Roma, Italy*

[2]*Dipartimento di Chimica Fisica "M. Rolla," INSTM and IENI-CNR, Università di Pavia, Viale Taramelli 16, I-27100 Pavia, Italy*

(Received 17 November 2006; published 10 May 2007)

Raman and combined infrared transmission and reflectivity measurements were carried out at room temperature (RT) on monoclinic VO_2 over the 0–19 GPa and 0–14 GPa pressure ranges. Both lattice dynamics and optical gap show a remarkable stability up to $P^* \sim 10$ GPa whereas subtle modifications of V ion arrangements within the monoclinic lattice, together with the onset of a metallization process via band gap filling, are observed for $P > P^*$. Differently from $P = 0$, where the VO_2 metallic phase is found only in conjunction with the rutile structure above 340 K, a new RT metallic phase within a monoclinic structure appears accessible in the high pressure regime.

DOI: 10.1103/PhysRevLett.98.196406 PACS numbers: 71.30.+h, 62.50.+p, 63.20.Kr, 78.30.−j

Since the first observation of the metal-insulator transition (MIT) in vanadium oxides, these materials have attracted considerable interest because of the abrupt and often huge change of conductivity at the MIT. As usual in transition metal oxides, electronic correlation strongly affects the conduction regime, although, in some V-oxides, lattice degrees of freedom seem also to play an important role. This is the case of VO_2, which undergoes a first order transition from a high temperature metallic rutile (R) phase to a low temperature insulating monoclinic ($M1$) one. At the MIT temperature, $T_c = 340$ K, the opening of a gap in the midinfrared (MIR) optical conductivity and a jump of several order of magnitude in the resistivity are observed [1]. The interest in this compound is mainly focused on understanding the role and the relative importance of the electron-electron and the electron-lattice interaction in driving the MIT. Despite the great experimental and theoretical efforts [2], the understanding of this transition is still far from being complete [3–7]. In the metallic R phase, the V atoms, each surrounded by an oxygen octahedron, are equally spaced along linear chains in the c-axis direction and form a body-centered tetragonal lattice. On entering the $M1$ insulating phase, the dimerization of the vanadium atoms and the tilting of the pairs with respect to the c axis lead to a doubling of the unit cell, with space group changing from D_{4h}^{14} (R) to C_{2h}^{5} ($M1$) [8,9]. As first proposed by Goodenough [10], the V-V pairing and the off-axis zigzag displacement of the dimers lead to a band splitting with the formation of a Peierls-like gap at the Fermi level. First principle electronic structure calculations based on local density approximation (LDA) showed the band splitting on entering the $M1$ phase, but failed to yield the opening of the band gap [11,12]. As early pointed out [13], the electron-electron correlation has to be taken into account to obtain the insulating phase. A recent paper where the electronic Coulomb repulsion (U) is properly accounted for shows that calculations based on dynamical mean field theory within the LDA scheme correctly captured both the metallic R and the insulating $M1$ phases [4].

There are many experimental evidences of strong electronic correlation in VO_2, as, e.g., the anomalous linear temperature dependence of conductivity above T_c up to 800 K [14]. Moreover, a recent study of the temperature dependence of the optical conductivity, $\sigma_1(\omega)$, [6] shows that MIT involves a redistribution of spectral weight [i.e., the frequency-integrated $\sigma_1(\omega)$] within a broad energy scale ($\geq$5.5 eV). This suggests electronic correlation to be crucial for the MIT, even though the insulating state may not be a conventional Mott insulator because of the Peierls pairing. Finally, it should be noted that insulating monoclinic VO_2 with a different space group C_{2h}^{3} ($M2$) can be achieved under peculiar growing condition [15] as well as by means of minute amounts of Cr/V substitution [16]. In the $M2$ phase, the Peierls pairing is partially removed: one half of the V atoms dimerizes along the c-axis, and the other one forms zigzag chains of equally spaced atoms [16]. The insulating character of the $M2$ phase supports the idea that the physics of VO_2 is close to that of a Mott-Hubbard insulator [17].

High pressure (HP) is an ideal tool for studying electron-correlated systems. Lattice compression usually increases the orbital overlap and the electronic bandwidth (W), thus allowing for a systematic study of the physical properties as a function of U/W. Unfortunately, there is an almost complete lack of HP data on VO_2 apart from early resistivity measurements which show a small pressure-induced increase ($\sim$3 K) of T_c in the 0–4 GPa range [18]. On the contrary, a remarkable decrease ($\sim$20 K) of T_c within the 0–5 GPa range was observed in Cr-doped VO_2 in the $M2$ phase [16].

Here, we report on HP Raman (0–19 GPa) and MIR (0–14 GPa) measurements on VO_2 at room temperature (RT) to study pressure-induced effects on both lattice dynamics and electronic structure. In particular, since the optical gap lies in the MIR region and the Raman spectra of VO_2 are drastically different in the R and $M1$ phases, these techniques allow us to independently monitor the electronic and the structural transitions. VO_2 was prepared starting

from V_2O_3 and V_2O_5 (Aldrich >99.9%), pressed into pellets and reacted at 1050 °C in an Ar flux for 12 h. A pure $M1$ monoclinic structure was observed by RT x-ray diffraction on some crystals and a powdered sample. Differential Scanning Calorimetry on synthesized samples revealed a clear endothermic peak at about 340 K in agreement with the known T_c value. A screw clamped opposing-plates diamond anvil cell (DAC) equipped with 400 μm culet II A diamonds, was used for both Raman and MIR experiments. The gaskets were made of a 250 μm thick steel foil with a sample chamber of 130 μm diameter and 40 to 50 μm height under working conditions. We used NaCl an KBr as pressure transmitting media for Raman and MIR measurements, respectively [19,20], and the ruby fluorescence technique for the determination of the pressure.

HP MIR spectra of RT VO_2 were collected exploiting the high brilliance of SISSI infrared beam line at ELETTRA synchrotron in Trieste [21]. The incident and reflected (transmitted) radiation were focused and collected by a cassegrain-based Hyperion 2000 infrared microscope equipped with a MCT detector and coupled to a Bruker IFS 66v interferometer, which allows us to explore the 750–6000 cm^{-1} spectral range. A VO_2 5 μm thick slab, obtained by pressing finely milled sample between the diamond anvils, was placed in the gasket hole, where a KBr pellet was previously sintered [22]. This procedure allows us to measure a sample slab with sharp surfaces and well defined thickness [22]. The slits of the microscope, adjusted to collect transmitted and reflected light from the sample only, were kept fixed during the experiment.

The high brilliance of the infrared synchrotron source and the proper sample thickness allow us to measure the intensities reflected, $I_R^S(\omega)$, and transmitted, $I_T^S(\omega)$, at each pressure. Possible misalignments and source intensity fluctuations were accounted for by measuring the intensity reflected by the external face of the diamond anvil, $I_R^D(\omega)$, at each working pressure. At the end of the pressure run, we measured the light intensities reflected by a gold mirror placed between the diamonds $I_R^{\mathrm{Au}}(\omega)$ and by the external face of the diamond anvil $I_R^{D\prime}(\omega)$. By using the ratio $I_R^{D\prime}(\omega)/I_R^D(\omega)$ as a correction function, we achieved the reflectivity $R(\omega)$:

$$R(\omega) = \frac{I_R^S(\omega)}{I_R^{Au}(\omega)} \frac{I_R^{D\prime}(\omega)}{I_R^D(\omega)}. \quad (1)$$

The transmittance $T(\omega)$ was obtained using

$$T(\omega) = \frac{I_T^S(\omega)}{I_T^{\mathrm{DAC}}(\omega)} \frac{I_R^{D\prime}(\omega)}{I_R^D(\omega)} \quad (2)$$

where $I_T^{\mathrm{DAC}}(\omega)$ is the transmitted intensity of the empty DAC without gasket and with the anvils in tight contact. $R(\omega)$ and $T(\omega)$ at selected pressures are shown in Fig. 1.

At $P \sim 0$, the low-frequency reflectivity is characterized by a steep rise due to a phononic contribution, whereas, on the high-frequency side, $R(\omega)$ is slowly varying between

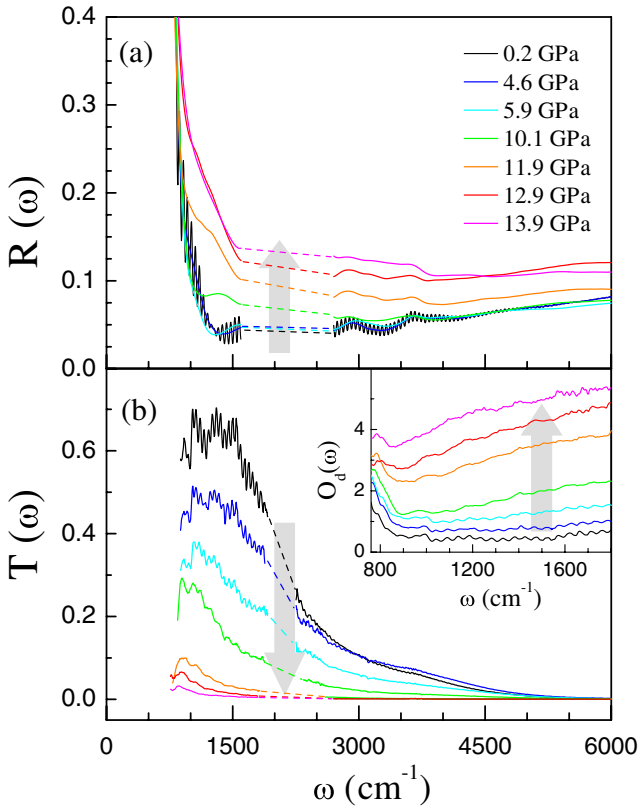

FIG. 1 (color online). (a) MIR reflectivity $R(\omega)$ and (b) transmittance $T(\omega)$ of VO_2 at selected pressures. Fringes were averaged out in the reflectivity spectra, except at the lowest pressure. Arrows indicate increasing pressure. Dashed lines replace the data at the frequencies where the diamond absorption is very high. Inset: correspondingly low-frequency optical density $O_d(\omega)$.

0.05 and 0.08, which is slightly higher than expected for sample-diamond interface [23,24]. The extra reflectivity is due to multiple reflections within the sample-KBr bilayer which also originate the interference fringes well evident in both $R(\omega)$ and $T(\omega)$. The low $T(\omega)$ values at high-frequency are due to the absorption of the low-frequency tail of the electronic band [6,24].

Within the 0–10 GPa range, $R(\omega)$ does not change remarkably whereas $T(\omega)$ gradually decreases. On increasing pressure above 10 GPa, $R(\omega)$ starts to increase and $T(\omega)$ abruptly decreases to very small values owing to the shift of the electronic band towards lower frequencies. The optical density $O_d(\omega) = -\ln T(\omega)$, shown in the inset of Fig. 1, makes evident this process: above 10 GPa, the electronic contribution fills the optical gap, and the phonon peak is remarkably screened, thus showing the onset of a pressure-induced charge delocalization process.

The simultaneous measurement of $R(\omega)$ and $T(\omega)$ enables us to extract the real, $n(\omega)$, and the imaginary, $k(\omega)$, part of the complex refractive index of VO_2. To this purpose, thanks to the present loading procedure, a multilayer scheme diamond-sample-KBr-diamond was adopted, where multiple reflections within the sample and the KBr

layers were accounted for by adding incoherently the intensities of the reflected beams [25]. Using the experimental layer thickness and the known optical properties of diamond [23] and KBr [26], $R(\omega)$ and $T(\omega)$ can be expressed as a function of $n(\omega)$ and $k(\omega)$ only. The analytical derivation, under the above assumptions, is straightforward albeit rather lengthy and is being reported in a forthcoming paper. $n(\omega)$ and $k(\omega)$ were thus obtained by a numerical iterative procedure[27]. The results obtained at the lowest pressure are in good agreement with literature data at $P = 0$ [6,24]. The optical conductivity $\sigma_1(\omega) = 2\omega/4\pi \cdot n(\omega)k(\omega)$ is shown in Fig. 2 at different pressures . The low-frequency region of the spectra was not reported because the strong variations of the optical constants around the phonon contribution could affect the reliability of the iterative procedure. The data shown in Fig. 2 allow us to follow the pressure behavior of the low-frequency tail of the electronic band, which is the spectral structure mostly affected by the MIT [6].

At $P \sim 0$, $\sigma_1(\omega)$ is in good agreement with ambient pressure data [6], and it is weakly pressure dependent up to 4 GPa. On further increasing the pressure, $\sigma_1(\omega)$ progressively increases, mainly within the 1500–4500 cm^{-1} frequency range. Above 10 GPa, the overall $\sigma_1(\omega)$ abruptly increases and a remarkable pressure-induced band gap filling is observed. The data at the highest pressure clearly show that the energy gap, if still open, is well below 900 cm^{-1}. We notice that a rough linear extrapolation of the data collected at $P > 10$ GPa gives positive, although small, $\sigma_1(\omega = 0)$ values compatible with a bad metal behavior.

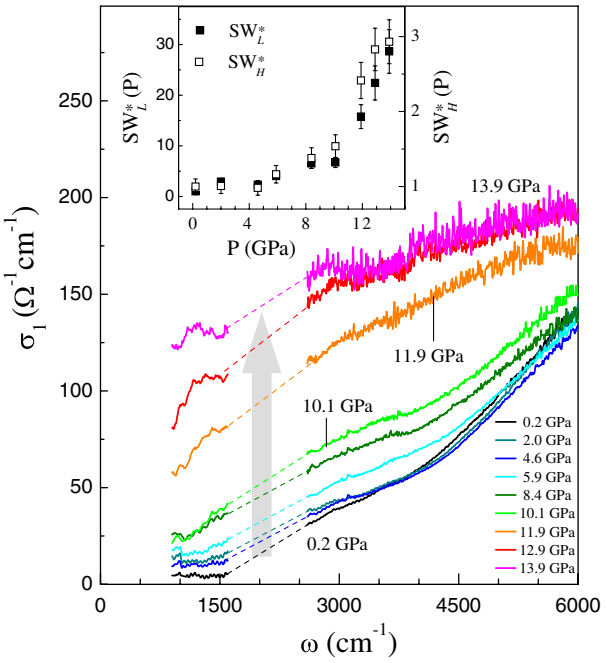

FIG. 2 (color online). Optical conductivity $\sigma_1(\omega)$ of VO_2 at different pressures. Dashed lines are guides to the eyes. Inset: normalized spectral weights $SW_L^*(P)$ and $SW_H^*(P)$.

The effect of pressure is clarified by analyzing the pressure dependence of the spectral weight SW(P). At each pressure, we calculated the frequency integral of $\sigma_1(\omega)$ over 900–1600 cm^{-1} [$SW_L(P)$] and 2600–5000 cm^{-1} [$SW_H(P)$]. The integration was not extended above 5000 cm^{-1}, owing to the onset of saturation effects in the spectra collected at the highest pressures (see in Fig. 2 the high noise level at high frequencies). The spectral weights normalized to the lowest pressure values, $SW_L^*(P) = SW_L(P)/SW_L(0)$ and $SW_H^*(P) = SW_H(P)/SW_H(0)$, are shown in the inset of Fig. 2. Both the SW(P) show the same dependence, with an abrupt change of slope at 10 GPa. We notice that the absolute pressure-induced variation of $SW_L^*(P)$ is much larger than that observed for $SW_H^*(P)$, as expected if charge delocalization occurs [6]. Such a large and abrupt increase of the spectral weight in the gap region is certainly compatible with the occurrence of a pressure-induced MIT, although the spectral range of the present measurements does not allow us to claim undoubtedly the complete optical gap closure above 10 GPa.

Raman measurements were carried out using a confocal micro-Raman spectrometer equipped with a He-Ne laser source (632.8 nm), a 1800 g/cm grating, and a CCD detector. A notch filter was used to reject the elastic contribution of the backscattered light collected by a 20x objective. Under these experimental conditions, we achieved a few microns diameter laser spot on the sample and a spectral resolution of 3 cm^{-1}. The absence of strong pressure-gradients was tested by collecting Raman spectra from different points over a flat surface (50×50 μm^2) of a small crystal. The reduced dimension and the irregular shape of the sample did not allow for accurate alignment. The Raman spectra of VO_2 at selected pressures are shown in Fig. 3. The spectrum at the lowest pressure is in full agreement with previous ambient pressure Raman data on VO_2 in the $M1$ phase [28,29]. Fifteen narrow phonon peaks of the 18 Raman-active modes predicted for the $M1$ phase ($9A_g + 9B_g$) can be identified in the present measurements. The effect of applied pressure on the Raman spectrum results in a phonon frequency hardening, which, however, does not significantly changes either the peak pattern or the overall spectral shape. Variations of the relative intensities of phonon peaks must be ascribed to polarization effect, particularly strong in VO_2 [29]. Since the Raman spectrum of VO_2 in the R phase is characterized by 4 broad peaks only [28,29], we can safely conclude at a glance that a transition to a R phase is not achieved by applying pressure up to 19 GPa. The good quality of the data allows us to apply a standard fitting procedure [19] to analyze the pressure dependence of the phonon spectrum. The analysis shows an almost linear increase of the frequencies of every phonon peak except for the ω_{V1} and ω_{V2} peaks at 192 cm^{-1} and 224 cm^{-1} at $P \sim 0$, respectively, whose pressure dependence is shown in the inset of Fig. 3. A rather abrupt change of the rate $d\omega/dP$ from a value

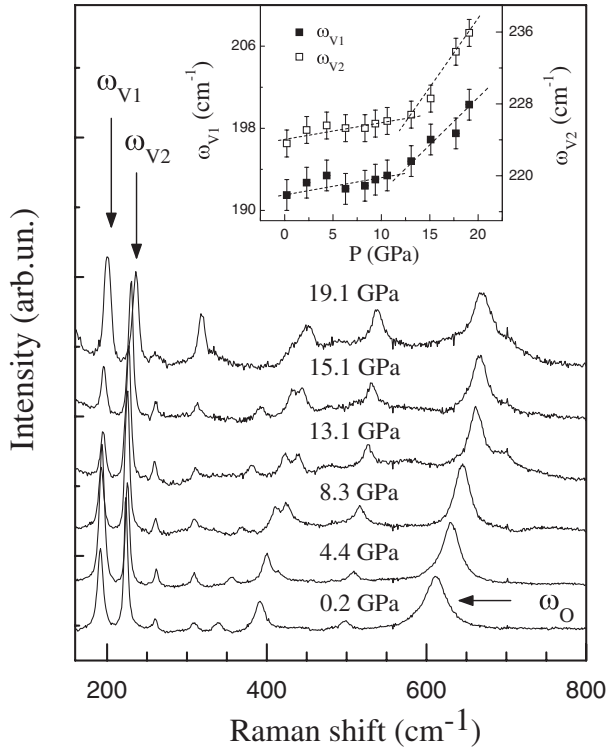

FIG. 3. Raman spectra of VO_2 at different pressures. Arrows mark the phonon peaks ω_{V1}, ω_{V2}, and ω_O. Inset: pressure dependence of ω_{V1} and ω_{V2} (dashed lines are guide to the eyes).

close to zero to 1–1.5 cm^{-1}/GPa is apparent at $P \sim$ 10 GPa.

Because of the large difference between V and O masses, the low-frequency ω_{V1} and ω_{V2} peaks can be ascribed to the V-ions motion in the dimerized chains. In fact, by comparing the phonon frequencies of VO_2 with those of the isostructural NbO_2, which exhibits a similar Raman spectrum [30], ω_{V1} and ω_{V2} frequencies scale with the mass of the transition metal, while the frequency of the ω_O peak (see Fig. 3) scales with the reduced mass of the oxygen and the transition metal. Albeit the monoclinic structure is retained over the whole pressure range, the latter finding suggests a rearrangement of the V-V dimers as the pressure is increased above 10 GPa.

To summarize, we report on a HP Raman and MIR investigation of VO_2. In particular, taking full advantage from the high brilliance of the SISSI beam line, we were able to collect both transmittance and reflectivity of the sample inside the DAC allowing for a full analysis of the MIR data. The whole of the results clearly identifies two regimes, below and above a threshold pressure $P^* \sim$ 10 GPa. Both Raman and IR spectra show a weak pressure dependence for $P < P^*$, whereas for $P > P^*$ the pressure-driven optical gap filling is accompanied by a rearrangement of the V-chains within a monoclinic framework. The stability of the monoclinic phase, which is retained up to 19 GPa, and the pressure-driven delocalization process, which starts at P^* and is remarkable at the highest pressures, indicate that the MIT and the $M1$-R transition are decoupled in HP VO_2. It is worthwhile to notice that new HP x-ray diffraction data [31] extend the stability of the monoclinic phase up to 42 GPa.

The onset of a metallic monoclinic phase apparently rules out the role of the Peierls distortion in the MIT. However, the rearrangement of the V-chains at P^* suggests a subtle structural transformation toward a new monoclinic phase where the extent of Peierls-induced dimerization is still unknown, and V-chains can coexist with V-dimers as in the $M2$ phase [16]. The present results thus open new experimental quests and represent a severe benchmark for theoretical models aimed at addressing the role of electron-electron correlations and lattice structure in driving the MIT in VO_2.

[1] F. J. Morin, Phys. Rev. Lett. **3**, 34 (1959).
[2] M. Imada *et al.*, Rev. Mod. Phys. **70**, 1039 (1998).
[3] H. T. Kim *et al.*, New J. Phys. **6**, 52 (2004).
[4] S. Biermann *et al.*, Phys. Rev. Lett. **94**, 026404 (2005).
[5] H. S. Choi *et al.*, Phys. Rev. B **54**, 4621 (1996).
[6] M. M. Qazilbash *et al.*, Phys. Rev. B **74**, 205118 (2006).
[7] M. W. Haverkort *et al.*, Phys. Rev. Lett. **95**, 196404 (2005).
[8] D. B. McWhan *et al.*,Phys. Rev. B **10**, 490 (1974).
[9] J. M. Longo *et al.*, Acta Chem. Scand. **24**, 420 (1970).
[10] J. B. Goodenough, J. Solid State Chem. **3**, 490 (1971).
[11] R. M. Wentzcovitch *et al.*, Phys. Rev. Lett. **72**, 3389 (1994).
[12] V. Eyert, Ann. Phys. (Berlin) **11**, 650 (2002).
[13] A. Zylbersztejn *et al.*, Phys. Rev. B **11**, 4383 (1975).
[14] P. B. Allen *et al.*, Phys. Rev. B **48**, 4359 (1993).
[15] J. Galy and G. Miehe, Solid State Sci. **1**, 433 (1999).
[16] M. Marezio *et al.*, Phys. Rev. B **5**, 2541 (1972).
[17] T. M. Rice *et al.*, Phys. Rev. Lett. **73**, 3042 (1994).
[18] C. N. Berglund *et al.*, Phys. Rev. **185**, 1034 (1969).
[19] A. Congeduti *et al.*, Phys. Rev. Lett. **86**, 1251 (2001).
[20] A. Congeduti *et al.*, Phys. Rev. B **63**, 184410 (2001).
[21] S. Lupi *et al.*, J. Opt. Soc. Am. B **24**, 959 (2007).
[22] A. Sacchetti *et al.*, Phys. Rev. Lett. **96**, 035503 (2006).
[23] *Handbook of Optical Constants of Solids II*, edited by E. D. Palik (Academic, San Diego, 1991).
[24] H. W. Verleur *et al.*, Phys. Rev. **172**, 788 (1968).
[25] M. Dressel and G. Grüner, *Electrodynamics of Solids* (Cambridge University Press, Cambridge, England, 2002).
[26] P. G. Johannsen *et al.*, Phys. Rev. B **55**, 6865 (1997).
[27] The guess function $n^0(\omega)$ is set at the average value of the RT refraction index of VO_2 [24], and $k^0(\omega)$ is then derived from the $T(\omega)$ equation. The successive iterate, $n^1(\omega)$, is obtained inserting $k^0(\omega)$ into $R(\omega)$ and in turn $n^1(\omega)$ into $T(\omega)$ to get $k^1(\omega)$. The procedure is iterated till convergence. The results are independent of the guess function and agree with what obtained following Ref. [5].
[28] R. Srivastava *et al.*, Phys. Rev. Lett. **27**, 727 (1971).
[29] P. Schilbe, Physica (Amsterdam) **B316**, 600 (2002).
[30] Y. Zhao *et al.*, J. Phys. D **37**, 3392 (2004).
[31] L. Malavasi (private communication).